The effect of chemical dispersant concentration on hydrocarbon mobility through permeable North-East Scotland sands

Luis J. Perez Calderon[a,b,c], Lloyd D. Potts[a,b], Thomas Cornulier[a], Alejandro Gallego[c], James A. Anderson[b], Ursula Witte[a]

Institutional affiliations:

    a) Institute of Biological and Environmental Science, University of Aberdeen, Aberdeen, United Kingdom

    b) Surface Chemistry and Catalysis Group, Materials and Chemical Engineering, Department of Engineering, University of Aberdeen, Aberdeen, United Kingdom

    c) Marine Scotland Science, Marine Laboratory Aberdeen, Aberdeen, United Kingdom

Corresponding author: Luis J. Perez Calderon – lj.perezcalderon@gmail.com

Notes: Colour should be included for Figures 1, 2, 4 and 5.

Author contributions: LJP, JA and UW conceived the experiment. LJP and LDP collected the samples and carried out the experiment. LJP and TC analysed the data. All authors reviewed the manuscript.

Competing interests: The authors declare no competing interests.

Potential referees:

- Markus Huettel (Email: mhuettel@fsu.edu; Department of Earth, Ocean and Atmospheric Science, Florida State University, 117 N Woodward Av., Tallahassee, Florida 32306-4320; Website: http://myweb.fsu.edu/mhuettel/)
- Antje Rusch (Email: rusch@micro.siu.edu; Address: Southern Illinois University, Department of Microbiology, Life Science II 191; Website: http://micro.siu.edu/faculty-staff/faculty/rusch.php)
- Dongye Zhao (Email: zhaodon@auburn.edu; Address: Department of Civil Engineering, 209 Harbert Engineering Center, Auburn University, AL 36849-5337; Website: http://www.eng.auburn.edu/users/dzhao/)

28   • Helen K. White (Email: hwhite@haverford.edu; Address: 370 Lancaster Avenue,

29   Haverford, PA 19041; Website: https://www.haverford.edu/users/hwhite)

Highlights:

31   • Chemical dispersant increased the mobility of hydrocarbons through permeable sands.

32   • Chemical dispersant enhanced entrainment of oil below manufacturer recommended

33   dosing.

34   • Chemical dispersant selectively entrained hydrocarbons based on their solubility in

35   water.

Abstract:

37   Accidental releases of oil to the marine environment can reach sensitive shorelines resulting in

38   a wide range of environmental impacts. Chemical dispersant is a response tool employed to

39   minimise damage to coastal ecosystems by facilitating dispersal of oil slicks before they reach

40   shores. However, chemical dispersants may increase entrainment of hydrocarbons into coastal

41   sediments following an oil spill, resulting in higher hydrocarbon residence times in sediments.

42   Here, the effect of dispersant concentration on the entrainment capability of hydrocarbons in

43   permeable coastal sands from North East Scotland (United Kingdom) was evaluated.

44   Hydrocarbon entrainment into sands was facilitated by dispersant application at concentrations

45   below manufacturer-recommended dosage. Percolation of water-soluble hydrocarbons beyond

46   10 cm deep was not affected by chemical dispersant application and water-insoluble

47   component concentrations increased with dispersant concentration. Results highlighted that the

48   application of dispersant readily mobilised less water-soluble hydrocarbons through coastal

49   sands but did not affect pore-water transport of more water-soluble hydrocarbons.

Keywords: oil, transport, percolation, sediment, dispersant

1   Introduction

52   Accidental oil releases to the marine environment result in a wide variety of environmental

53   impacts. These are partly determined by the extent to which the oil evaporates, disperses and

54   biodegrades in the water column, settles on the seabed and reaches shores, among other fates

55   (Bandara et al., 2011; Davies and Tibbetts, 1987; Ramseur, 2010). Documented accidents such

56   as the *Deepwater Horizon* (*DwH*), *Prestige* and *Exxon Valdez* oil spills resulted in extensive

57 coastal oiling and subsequent environmental impacts which are detectable to this day (Beyer
58 et al., 2016; Levine et al., 2017; Payne et al., 2008).

59 Chemical dispersants were widely used during *DwH* response operations in an attempt to
60 mitigate its environmental impacts, with 5.3 million litres of dispersant applied at the sea
61 surface and 2.9 million litres at the wellhead (~1500 m deep). Dispersant use remains
62 controversial but has been shown to be beneficial under specific circumstances (Prince 2015).
63 The aim of dispersant application is to disperse insoluble and persistent hydrocarbons by
64 dispersing and dissolving oil as small droplets to increase their surface area with the end goal
65 of accelerating physical, chemical and biological oil degradation (Fingas, 2002). Additionally,
66 dispersant was applied at the wellhead during *DwH* to facilitate the removal of volatile
67 hydrocarbons from surfacing oil and reduce the risks of uncontrolled ignition of volatile
68 hydrocarbons on surface waters and inhalation by oil spill responders (International
69 Association of Oil & Gas Producers, 2015). Dispersant increases oil bioavailability by
70 increasing its accessible surface area and enabling microbes to access and utilise oil faster
71 (Hazen et al., 2010). However, by increasing oil bioavailability, dispersant also facilitates the
72 uptake of hydrocarbons by fauna such as filter feeders, marine mammals, seabirds and
73 commercially harvested fish, and can thus result in negative effects for both the marine
74 environment and reach humans through accumulation in the food chain (Beyer et al., 2016).
75 Moreover, dispersants have been found to be toxic to marine organisms and be more persistent
76 than previously thought (White et al., 2012).

77 Dispersed oil, whether mechanically or chemically dispersed, that reaches shorelines can be
78 entrained into sediments where it can persist for decades and act as a reservoir from which
79 contaminants can enter the food chain (Payne et al., 2008). If polyaromatic hydrocarbons
80 (PAHs, hereafter) reach anoxic sediments biodegradation may be limited and consequently
81 higher PAH half-life in sediments could be expected (Widdel et al., 2010). Whilst the mobility
82 of PAHs is especially relevant due to their carcinogenicity and persistence, entrainment of
83 hydrocarbons from other fractions (such as aliphatics and Benzene, Toluene, Ethyl benzene
84 and Xylene, BTEX hereafter) is relevant as these have been shown to induce an environmental
85 response, particularly in microbial communities (Phelps and Young, 1999). BTEX components
86 are far more water-soluble than PAHs, potentially being carried into permeable sediments more
87 readily.

88 Oil contact with sediments is particularly undesirable because of the well-known
89 environmental impacts it causes, the difficulty involved in restoring habitats and the damage
90 to the reputation of the responsible party (Beyer et al., 2016; Zuijdgeest and Huettel, 2012).
91 Consequently, understanding the potential entrainment of spilled oil into sediments in coastal
92 environments is relevant. During *DwH*, the shorelines of Louisiana and other southern states
93 of the United States were severely affected by beached oil (Nixon et al., 2016). Zuijdgeest and
94 Huettel (2012) assessed the entrainment potential of mechanically and chemically dispersed
95 MC525 oil (using Corexit 9500A) and found that mobility of Total Petroleum Hydrocarbons
96 (TPH, hereafter) and PAHs was increased when a 1:100 Corexit 9500A to oil ratio was applied
97 due to Corexit increasing the solubility of hydrocarbons.

98 Over 70% of the seabed of the North Sea is characterised as fine sand (Paramor et al., 2009).
99 Sandy seabeds are highly permeable and therefore facilitate pore-water flushing. Permeable
100 continental shelf sediments contribute significantly to benthic biogeochemical cycling and
101 primary production (Huettel et al., 2014). This highlights the importance of understanding the
102 capability of hydrocarbons to entrain permeable sediments, which may affect upstream
103 ecological processes should a large-scale oil spill take place.

104 The aims of this work were to evaluate the potential of spilled hydrocarbons to be entrained
105 into permeable sands and the effect of concentration of a commercially available dispersant
106 stockpiled in the United Kingdom (Superdispersant-25, SD25 hereafter) on this process using
107 Schiehallion crude oil and a synthetic oil (model oil, hereafter). A synthetic oil was used as it
108 gives a good intermediate between a single hydrocarbon and a crude oil. Additionally, the use
109 of a synthetic oil enabled a constant mixture that could be replicated and compared between
110 experiments. A further objective was to elucidate if SD25 selectively mobilised components of
111 different fractions of hydrocarbons at increasing SD25 concentration. The hypotheses of this
112 study were: (1) The effects of SD25 on hydrocarbon entrainment into sediments would be
113 observable from below manufacturer recommended application doses, (2) increasing SD25
114 concentration would increase the entrainment of hydrocarbons and would be less effective in
115 facilitating entrainment of the more soluble components of the model oil (such as BTEX and
116 naphthalene) and (3) Oils would readily entrain permeable sands and may do so to different
117 extents due to the difference in composition of the Schiehallion crude and model oils.

118

2   Materials and methods

2.1   Study site

The present study was conducted using intertidal sandy sediment collected at the mouth of the Ythan estuary (57°18'25.2"N 1°59'13.2"W), which is located 10 km to the north of Aberdeen, North East Scotland (United Kingdom, Figure 1).

Figure 1. Location of sampling station (purple pin), Ythan estuary, North East Scotland, United Kingdom.

The estuary's intertidal area has been estimated at 1.85 km^2, with a tidal flushing time between <14 hours (Balls, 1994) and 5–12 days (Leach, 1971). The sampling location chosen for this study was at the front-face of the beach. Samples were collected on December 2015 using acrylic cores (internal diameter = 3.6 cm, length = 30 cm) (small cores, hereafter) for sediment analysis and percolation experiments. Further samples were collected using larger cores (internal diameter = 10 cm, length = 30 cm) (large cores, hereafter) to measure permeability.

5

133   Seawater was collected from the site and UV-filtered (0.5 µm filter). Salient salinity and *p*H of

134   water used were 35 and 7.5, respectively. The Ythan estuary has been chosen as the study site

135   for this work due to its proximity to oil and gas offshore installations in the North Sea. These

136   sands are representative of Scottish intertidal sands. Moreover, the Ythan Estuary is classified

137   as a Special Protection Area under Article 4.1 of the Birds Directive (79/409/EEC, code:

138   UK9002221, Natura 2000 network), highlighting the importance of understanding the

139   implications of oil beaching in this region.

2.2   *Sediment characterisation*

141   All analyses detailed below were conducted on three replicate cores each, which were sectioned

142   into four 2.5 cm sections (i.e. 0–2.5, 2.5–5, 5–7.5 and 7.5–10 cm). Each section was

143   homogenised and subsamples subsequently oven dried at 60°C for three days and mechanically

144   milled to ensure uniform grain size. Total carbon content (TC) was determined using an

145   NA2500 elemental analyser (Carlo Erba Instruments). Total organic carbon content (TOC) was

146   determined by acidification of sediment samples with 10% HCl acid, overnight drying at 60°C

147   and subsequent carbon content quantification. Total inorganic carbon (TIC) content was

148   determined as the difference between TC and TOC.

149   For analysis of grain size distribution, a separate set of subsamples was dried overnight at

150   105°C and subsequently sieved through decreasing mesh sizes (diameter = 2000, 1000, 500,

151   250, 125 and 63 µm). Statistical analyses for the particle size distribution were performed using

152   Gradistat v.8 (Blott and Pye, 2001).

153   Saturated hydraulic conductivity (K_s) was measured using a UMS KSat benchtop saturated

154   hydraulic conductivity instrument using the falling head method (Head, 1982). Three large

155   cores were divided into two sections of depth ranges 0–5 cm, and 5–10 cm. Sectioned sediment

156   samples were saturated with degassed, deionised water prior to recording of the K_s value to

157   ensure no air bubbles were retained within the sediment, which might otherwise distort the

158   measurement. Triplicate measurements were taken for each sample to ensure representative K_s

159   values. Permeability (k) was derived from K_s by the equation:

$$k = \frac{K_s\, m}{\rho\, g}$$

160

161   Where ρ and m are the water density (g cm^{-3}) and viscosity (g cm^{-1} s^{-1}), respectively, and g is

162   gravity (9.81 m s^{-2}).

2.3 Critical Micelle Concentration of Superdispersant-25

The apparent critical micelle concentration (CMC) of SD25 was measured following a similar approach to that used by Gong et al. (2014). Briefly, three stock solutions of SD25 in seawater were prepared (327 ± 1 mg l^{-1}) and these were diluted with several volumes of seawater and were measured for surface tension using a tensiometer (Attension, Sigma 700) fitted with a Du Noüy ring (triplicate measurements for each sample). Surface tension was then plotted against logSD25 concentration (mg l^{-1}). A value of zero was allocated to log(SD25 concentration=0) (mg l^{-1}) for the purposes of establishing the apparent CMC. Thereafter, the change in gradient was used as a boundary to calculate two linear regressions and establish their intersection point which was inferred to be the CMC (Gong et al., 2014).

2.4 Oils used in percolation experiments

A North Sea crude oil (Schiehallion) and a model oil were used in this investigation. The SARA analysis of the Schiehallion crude oil was undertaken externally (Intertek, ITS Testing Services, United Kingdom) and the mass percentage of the four fractions was found to be: saturates 51.33%, aromatics 32.20%, resins 14.87% and asphaltenes 1.5%. C_{10-30} were the most abundant hydrocarbon chain-lengths in the Schiehallion crude oil (Supplementary Figure 1). The model oil was composed of 21 hydrocarbons including BTEX, aliphatic, PAH and resin fractions (Ferguson et al., 2017). The model oil was based on the Schiehallion crude oil to enable a comparison to the crude and analyse the fate of all its components individually. The model oil contained hydrocarbons larger than C_8 because these are more readily deposited on the seabed. Details of the percentage composition by component and fraction can be found in Table 1.

Table 1. Synthetic oil composition and selected properties of its components. Octanol-water coefficients were obtained from literature: (a) Sangster et al. (1989), (b) Mackay et al. (2006), (c) ChemSpider website, (d) Sigma Aldrich website.

Hydrocarbon	Hydrocarbon class	Molecular weight (g mol^{-1})	Octanol-water coefficient (log K_{OW})	Percentage composition	Sonication extraction efficiency (%)	Liquid-liquid extraction efficiency (%)
Ethyl-Benzene	BTEX (18.0%)	106.165	3.15[b]	6.1	97.4 ± 0.1	88.5 ± 7.3
m-Xylene		106.165	3.20[b]	6.0	97.9 ± 0.1	88.7 ± 7.2
o-Xylene		106.165	3.12[b]	5.9	99.3 ± 0.7	89.5 ± 7.0
Decane	Aliphatics (58%)	142.282	6.25[a]	9.0	99.1 ± 0.0	89.2 ± 7.0
1-Decene		140.266	4.70[b]	9.1	98.2 ± 0.6	88.7 ± 7.2
Dodecane		170.334	6.80 ± 1.00[a]	9.0	99.9 ± 0.0	89.4 ± 7.1
Tetradecane		198.388	8.00[a]	9.2	100.3 ± 0.1	88.7 ± 6.9
Pentadecane		212.415	7.50[b]	6.2	101.0 ± 0.2	89.0 ± 7.0
Hexadecane		226.441	8.00[b]	8.8	101.2 ± 0.2	88.3 ± 6.8
Heptadecane		240.468	8.50[b]	1.5	101.1 ± 0.0	88.7 ± 7.1
1-Octadecene		252.478	9.81[c]	1.4	101.2 ± 0.7	88.0 ± 6.9
Eicosane		282.547	10.0[b]	1.6	101.6 ± 0.5	87.5 ± 7.2
Docosane		310.601	12.44[c]	1.4	101.8 ± 0.4	88.1 ± 7.0
Tetracosane		338.654	12.0[b]	1.5	102.4 ± 0.2	87.8 ± 7.8
Naphthalene	PAHs (18.2%)	128.171	3.43[b]	5.4	99.9 ± 0.7	89.3 ± 6.9
Fluorene		166.219	4.18[a]	3.1	101.1 ± 0.4	89.3 ± 6.2
Phenanthrene		178.229	4.52[a]	3.0	100.4 ± 1.3	89.2 ± 6.0
Anthracene		178.229	4.50[a]	0.7	84.9 ± 4.0	86.9 ± 6.4
Fluoranthene		202.251	5.20[a]	3.1	101.7 ± 1.0	89.7 ± 6.4
Pyrene		202.201	5.17[c]	3.0	101.8 ± 1.1	89.6 ± 6.5
Dibenzothiophene	Resin (4.9%)	184.257	4.38[a]	4.9	101.0 ± 1.7	89.2 ± 6.4

2.5 Percolation experimental set-up

Solutions of SD25 in seawater were prepared by adding SD25 to seawater in one-litre volumetric flasks. Thereafter, SD25-seawater solutions were magnetically stirred at room temperature for 24 h to allow equilibration of SD25 in seawater. Immediately before percolations were performed, 100 ml of each solution was spiked with 1 g of oil and sonicated (45 kHz) in a USC-TH Ultrasonic bath (VWR) for 3 min to produce a proxy oil in water mixture to emulate the consequences of mechanical mixing of oil and water by waves and tides. The percolation experiment was based on a short column experiment by Zuijdgeest & Huettel (2012) with some modifications (Figure 2).

199
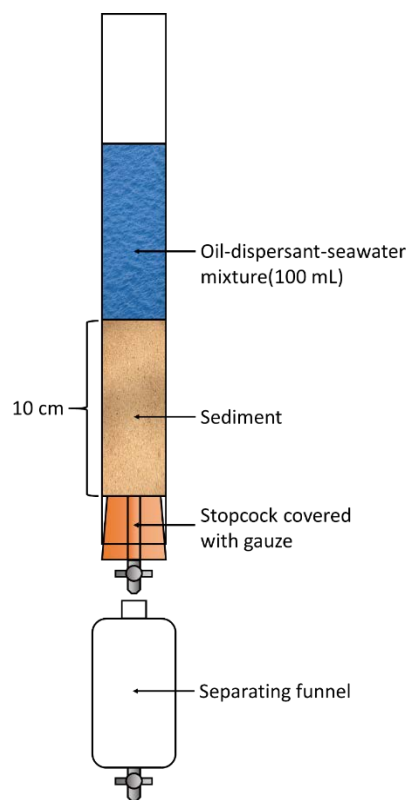
Figure 2. Percolation experiment setup.

Samples were extruded from the small cores used for collection and transferred to Pyrex cores of the same dimensions. Care was taken to avoid alteration to the sedimentary structure. The cores were then fitted with a gauze-lined stopcock to prevent blockage by sand. Sediment in cores was then saturated with uncontaminated seawater, after which mixtures of oil and SD25 at various concentrations (Table 2) were added to the cores avoiding sediment resuspension. The highest concentration (333.3 mg l^{-1}) corresponds to the lower boundary of the manufacturer's recommendations (1:30 dispersant to oil ratio). Immediately after the addition of the mixtures, the stopcock was opened to allow percolation of the mixtures through the sand until the water level reached the sediment surface. Washout water was collected and a further 100 ml of non-contaminated water were percolated through the cores using the same method. The combined washout oil-dispersant-seawater solution was collected in separating funnels and hydrocarbons were extracted within minutes. Sediment was then extruded and sectioned by depths (0.0–1.0, 1.0–3.0, 3.0–5.0, 5.0–7.5, 7.5–10.0 cm) for hydrocarbon extraction and analysis. The use of natural, undisturbed sediments was decided following preliminary experiments where mixed sand from the upper 10 cm were carried out and showed that mixing (homogenising) sand resulted in enhanced entrainment and therefore overestimated entrainment in Ythan estuary sands (Supplementary Figure 2).

218   Table 2. Superdispersant-25 (SD25) concentrations applied to the oils used.

Oil type	SD25 concentration (mg l^{-1})					
Control	0	-	-	-	-	-
Schiehallion crude oil	0	-	-	-	-	333.3
Synthetic oil	0	9.8	21.1	42.0	150	333.3

219

2.6 Hydrocarbon extraction and analysis

221   Hydrocarbon extractions from sediment were performed by sonicating each sediment section
222   in 50 ml of dichloromethane for 10 min for model oil-contaminated samples. The procedure
223   was performed in triplicate for the Schiehallion crude oil-contaminated sediment extractions.
224   Extractions from washout water were performed by liquid-liquid extraction with 3×25 ml
225   dichloromethane for both oil type-contaminated sediments. Hydrocarbons were quantified
226   against external standards containing known concentrations of the model oil components.
227   Hydrocarbon recovery efficiencies for each component can be found in Table 1. Schiehallion
228   crude oil extractions were subsequently rotary-evaporated at 40°C until all dichloromethane
229   had evaporated. Model oil extracts were analysed by gas chromatography (GC, hereafter) with
230   flame ionizing detection using a previously described system (Ferguson et al., 2017). When no
231   hydrocarbons were detected by GC, extracts were further concentrated by rotary evaporating
232   to 10 ml and reinjected into the GC. Schiehallion crude oil was analysed gravimetrically as
233   TPH.

234   Calibration curves (6-point) were determined for each compound of the model oil. Laboratory
235   control samples were analysed to establish the effect of the sediment matrix and extraction
236   procedure on the recovery of model oil compounds. Toluene was added (1 µl ml^{-1}) as an
237   internal standard to correct for injection error in the GC analysis. The limits of detection (LOD)
238   and quantification (LOQ) were defined as chromatographic signal to noise ratios (S:N) of 3
239   and 10, respectively. When chromatographic peaks had a S:N between the LOD and LOQ were
240   assigned a value of LOQ/2.

2.7 Chemicals

242   All model oil components (Table 1), toluene (99.8%), dichloromethane (99.8%) and hydrogen
243   peroxide (30%) were purchased from Sigma Aldrich. SD25 was purchased from Oil Technics
244   (Aberdeenshire). Sodium hexametaphosphate (technical grade) was purchased from Alfa
245   Aesar.

2.8 Calculations and statistical modelling

To establish valid comparisons across SD25 treatments, hydrocarbon concentrations in sediment were normalised to the total mass of hydrocarbon accounted for in all sediment layers and washout as follows:

$$C_{i,j,k} = \frac{\frac{m_{i,j,k}}{t_{i,k}}}{s_{j,k}}$$

Where $C_{i,j,k}$ is the normalised concentration in sediment of hydrocarbon i in section j in core k, $m_{i,j,k}$ is the mass of hydrocarbon i in section j in core k, $t_{i,k}$ is the total mass of hydrocarbon i in all sediment layers and washout of core k and $s_{j,k}$ is the mass of sediment in section j in core k. Washout hydrocarbon mass was normalised to total hydrocarbon mass in sediment and washout mixture as follows:

$$W_{i,k} = \frac{m_{i,k}}{t_{i,k}}$$

Where $W_{i,k}$ is the normalised mass of hydrocarbon i in the washout of core k and $m_{i,k}$ is the mass of hydrocarbon i in the washout mixture of core k. Depth and SD25 were expected to have non-linear effects and interactive effects on C. Therefore, a generalised additive mixed effects model (GAMM) was therefore fitted to the data including, for each individual hydrocarbon, a bivariate tensor product smooth of depth and SD25 (Wood, 2006). Core identity (k) and Hydrocarbon identity (i) were specified as crossed random intercepts which allowed for variation in average C between cores and between model oil components. A lag-1 continuous autoregressive residual correlation term was included in the model to account for the lack of independence between depth segments due to the movement of hydrocarbon from the surface of the sediment to the segments underneath, such that C at one depth segment was allowed to depend on C of the same hydrocarbon at the depth segment directly above it. Due to the much higher concentration of hydrocarbons in the 0–1 cm layer compared to the rest of the sediment column ($89.5 \pm 6.8\%$), the data from this layer was omitted from the GAMM. The response variable C was square root transformed prior to fitting the model to improve homoscedasticity of residuals, and a Gaussian distribution was assumed for the data. The model formula was:

$$C \sim te(z, \text{SD25}, \text{by} = \text{i})$$

274   Where C is normalised hydrocarbon concentration, *te* represents tensor product smooths, z is

275   the sediment depth (cm), *SD25* is SD25 concentration (mg l^{-1}), *by* estimates a separate smoother

276   for each hydrocarbon i. Assessment of W_i as a function of SD25 concentration was modelled

277   using locally weighted regression where W_i was the response variable and SD25 concentration

278   was the explanatory variable. The model fits a polynomial surface determined by SD25

279   concentration as a predictor using local polynomial regression fitting (Cleveland et al., 1992).

280   W_i and SD25 concentration were log-scaled for ease of visualisation. For comparisons between

281   Schiehallion and model oil, TPH mass percentages retained at each sediment depth and

282   washout a locally weighed regression was also used where mass percentage was the response

283   variable and depth was the explanatory variable. Models were developed for SD25

284   concentration = 0 and 333.3 mg l^{-1} separately, and mass percentage was log-scaled for ease of

285   visualisation. Where pair-wise comparisons were carried out, two-way ANOVAs are used to

286   establish if SD25 application and oil type showed significant effects. All statistical analyses

287   were carried out using the statistical software R (R Development Core Team, 2017) and the

288   libraries *ggplot2* (for the locally weighed regression analysis) and *mgcv* (for the GAMM

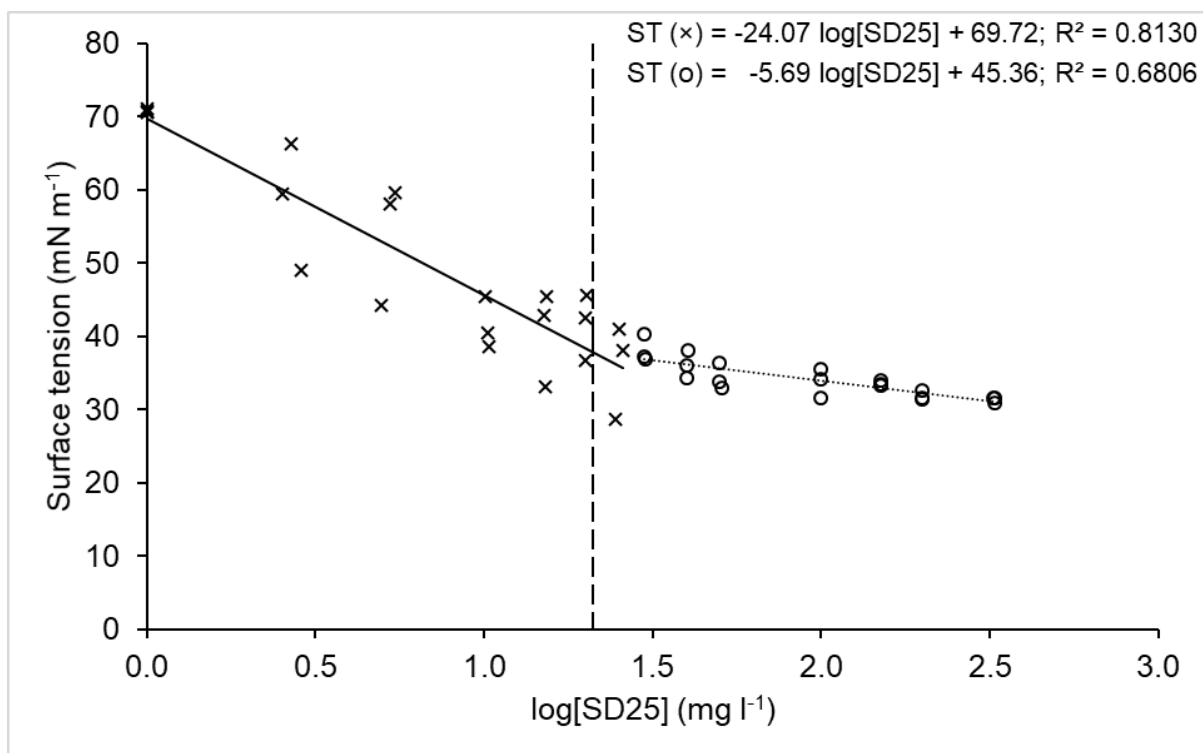289   analysis) (Wickham, 2009; Wood, 2011).

290

3 Results

3.1 Sediment properties and SD25 characterisation

The sediments analysed were classified as sands and were found to be highly permeable (Table 3). The intersection of linear response of surface tension to SD25 concentration, the apparent CMC of SD25 in seawater, as 21.1 mg l^{-1} (Figure 3).

Table 2. Ythan intertidal sediment characteristic. Permeability was measured at larger depth intervals than the other properties shown due to the size requirement of the instrument used. Errors represent standard deviation (n = 3). D50, TC, TIC and TOC refer to mass-median-diameter, total carbon, total inorganic carbon and total organic carbon, respectively.

|	Sediment size and sorting			Carbon content			Permeability	
Depth (cm)	D$_{50}$ (µm)	Sorting	TC (%)	TIC (%)	TOC (%)	Depth (cm)	Permeability (m^2)
0.0–2.5	299.1 ± 11.4	Moderately Well Sorted Medium Sand	0.072 ± 0.024	0.043 ± 0.028	0.029 ± 0.006	0.0–5.0	4.04 × 10^{-11} ± 2.25 × 10^{-12}
2.5–5.0	309.8 ± 6.6	Moderately Well Sorted Medium Sand	0.052 ± 0.045	0.038 ± 0.033	0.014 ± 0.012		
5.0–7.5	334.5 ± 20.3	Moderately Well Sorted Medium Sand	0.086 ± 0.012	0.061 ± 0.018	0.026 ± 0.006	5.0–10	4.54 × 10^{-11} ± 4.99 × 10^{-12}
7.5–10	328.7 ± 5.3	Slightly Very Fine Gravelly Medium Sand	0.038 ± 0.010	0.019 ± 0.008	0.019 ± 0.005		

Figure 3. Surface tension of Ythan seawater as a function of Superdispersant-25 (SD25) concentration to establish the apparent critical micelle concentration of SD25. Crosses and circles denote the separation of the dataset to calculate linear regressions (solid and dotted lines, respectively) from the change of slope and their intersection (vertical dashed line).

3.2 Model oil – Schiehallion crude oil comparison

The proportion of TPH retained in the top layer (0–1 cm) for model oil was significantly higher than that of Schiehallion crude oil aggregating treatments of both oil, and oil and dispersant treatments (89.5 ± 6.8% and 72.4 ± 16.9%, respectively, p-value = 0.04). Dispersant recommended dosage reduced the percentage to TPH retained in the top layer for model oil (95.1 ± 2.4% to 83.9 ± 4.1%, p = 0.01) but not for crude oil (79.9 ± 17.0% to 64.9 ± 16.1%, p = 0.33). Mass percentage decreased exponentially with depth for both oils and treatments. Locally weighed regressions revealed a clear increase in mass percentage as depth increased for model oil but not for crude oil when SD25 was applied at recommended dosage (Figure 4) SD25 did not have a consistent effect on the mass percentage of Schiehallion crude oil retained at any sediment layer but did increase the percentage of oil in the washout (3.7 ± 5.7% and 0% when SD25 was not applied).

14
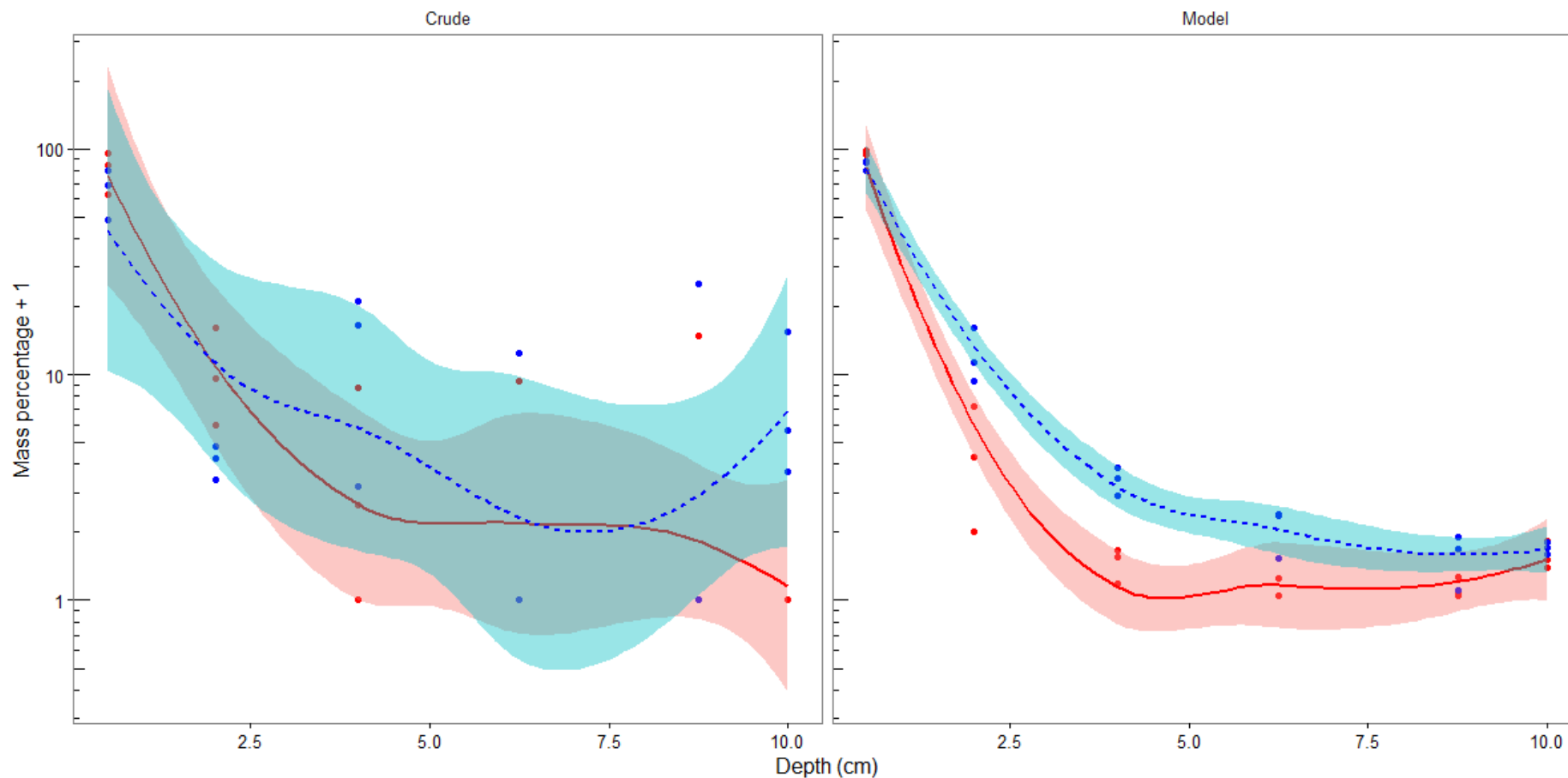
Figure 4. Total hydrocarbon mass percentage as a function of depth by treatment. Oils used were crude oil (left) and model oil (right) and treatments were oil only (red dots) and oil and 333.3 mg l^{-1} Superdispersant-25 (blue dots). Oil (red) and Oil and dispersant (blue) treatment lines bands represent locally-weighed regression values and associated standard errors, respectively. Note mass percentage has been log(x+1)-scaled.

3.3 Hydrocarbon entrainment into the top 10 cm of sediment

The GAMM results indicate that the application of SD25 increased the normalised concentration of all hydrocarbons with depth, even at SD25 concentration below the recommended dosing (Figure 5, Supplementary Figure 3, Supplementary Table 1). Overall, the application of SD25 increased the amount of oil entrained into these sands. The effect of SD25 was similar for most hydrocarbons in the top 4 cm. However, differences in the effect of SD25 on the entrainment of hydrocarbons became apparent at depths greater than 4 cm. C_{10-12} aliphatics showed a linear increase in entrainment with increasing SD25 concentration as in the surface layers. The remaining hydrocarbons showed increased entrainment into these sands at SD25 concentration above 42 mg l^{-1}. 1-Octadecene showed an unexpected response compared to equivalent length aliphatics (C_{17} and C_{19}) with no effect of SD25 concentration on entrainment over 5 cm deep. Dibenzothiophene, the only resin in the model oil, showed enhanced entrainment in sediments from low SD25 concentration. Interestingly, entrainment of dibenzothiophene did not increase with dispersant concentration in the range 150–333 mg SD25 l^{-1} at depths greater than 7 cm.
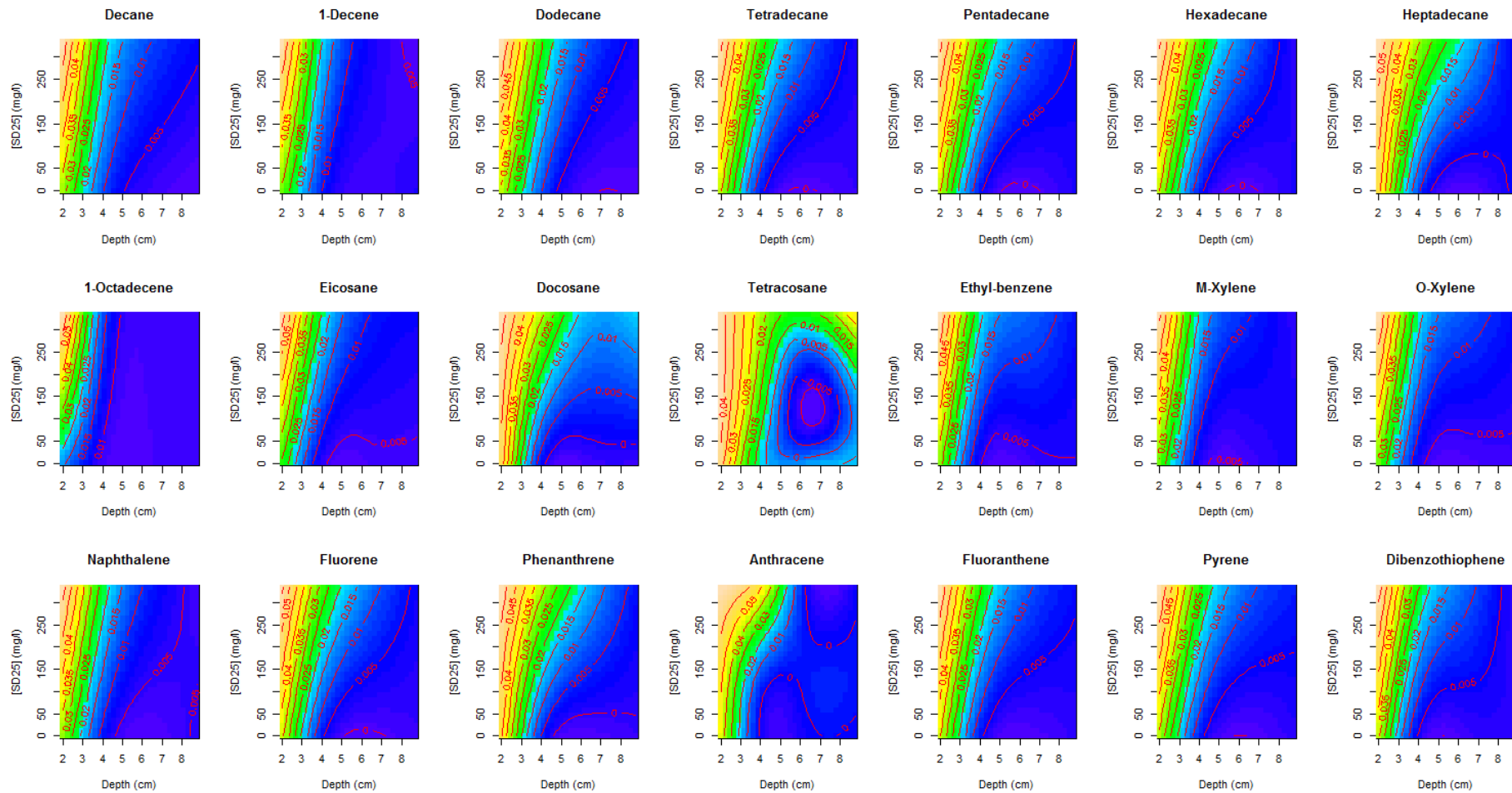
Figure 4. Generalised additive mixed effects models of hydrocarbon concentration in Ythan intertidal sands following percolation with increasing Superdispersant-25 concentrations from sediment depths of 1 to 10 cm. Note hydrocarbon concentrations have been normalised and square-rooted.

340 *3.4 Hydrocarbon entrainment beyond 10 cm of sediment*

341   W_i in the washout varied by component and SD25 concentration (Figure 6). For C_{10-14}

342   aliphatics, the influence of SD25 concentration on W_i was unclear. $W_{Pentadecane}$ (C_{15}) was

343   increased at 42 mg SD25 l^{-1} but higher concentrations did not result in further increases of

344   $W_{Pentadecane}$. $W_{Hexadecane}$ (C_{16}) increased with SD25 concentration. Heptadecane (C_{17}) and

345   tetracosane (C_{24}) showed a higher W_i at and above 21.1 mg SD25 l^{-1}. Interestingly, SD25

346   application did not affect $W_{1-Octadecene}$ (C_{18}) but affected C_{20} and C_{22} aliphatics which only

347   increased at SD25 concentration >150 mg l^{-1}. For the more soluble components of the model

348   oil such as BTEX and naphthalene, no clear effect of SD25 concentration was observed, with

349   W_i fluctuating as SD25 concentration increased. The response of fluorene to SD25

350   concentration was similar to that of C_{10-15} aliphatics, but with only a slight increase of $W_{Fluorene}$

351   at SD25 concentration above 21.1 mg l^{-1}. Larger PAHs showed increased W_i from 42 mg SD25

352   l^{-1} except anthracene which only showed increased $W_{Anthracene}$ at 333.3 mg SD25 l^{-1}, possibly

353   as a result of its lower percentage composition of the model oil. Dibenzothiophene, showed a

354   steady increase in $W_{Dibenzthiophene}$ with SD25 concentration.
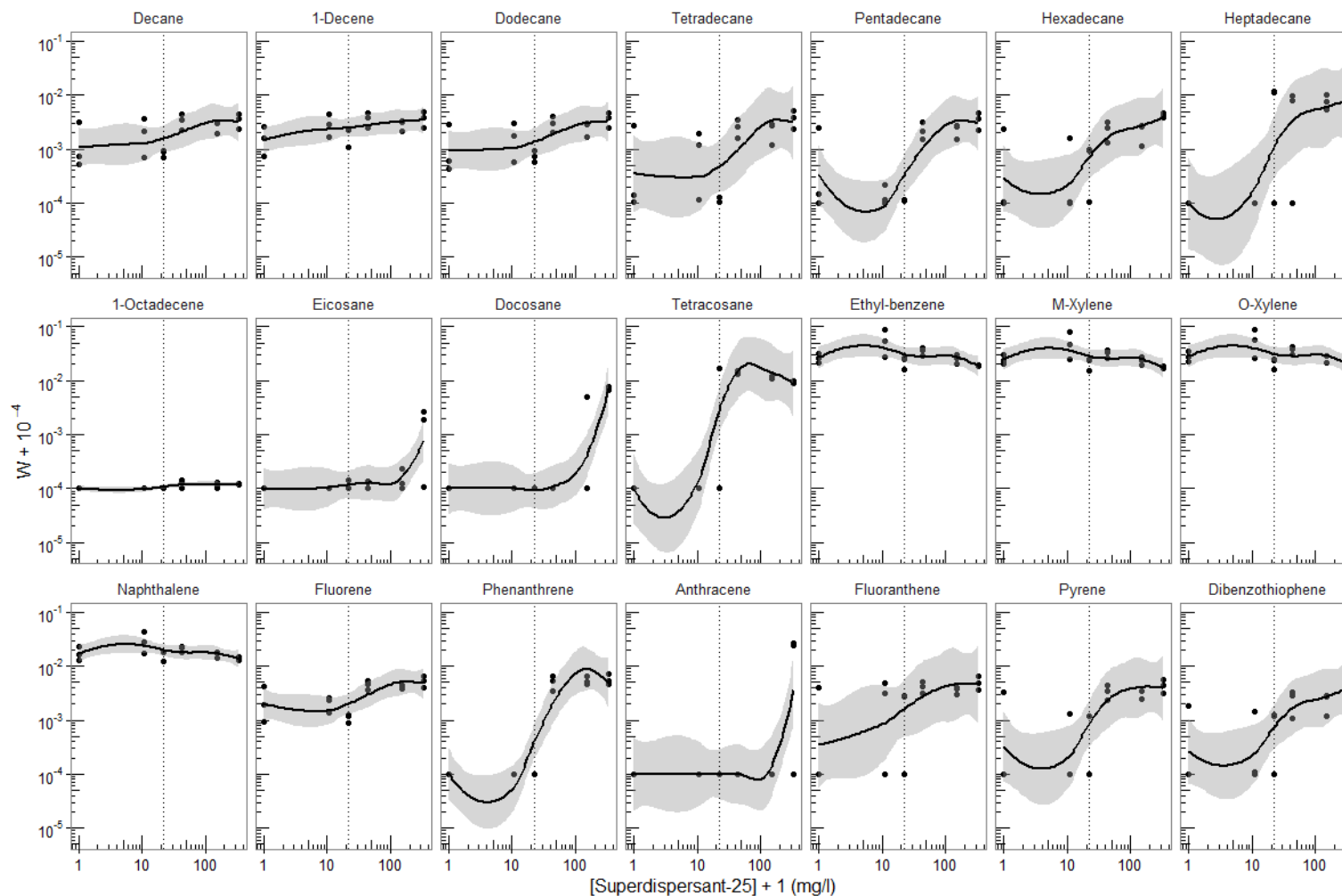
Figure 5. Normalised hydrocarbon mass in washout mixtures (*W*) as a function of Superdispersant-25 concentration. Points represent raw data and lines with grey bands represent locally-weighed regression values and associated standard errors, respectively. Note *W* and Superdispersant-25 concentration were $\log(x+10^{-4})$ and $\log(x+1)$-scaled, respectively.

4 Discussion

4.1 Key findings

SD25 application enhanced the mobility of hydrocarbons of the model oil through the top 10 cm of sediment and increased the W_i of leached hydrocarbons. The effect was most pronounced at and above 150 mg l^{-1} (half of the recommended dosage in terms of SD25:oil ratio) (Figures 5 and 6). The effect of SD25 application on W_i varied with hydrocarbon type, with BTEX and naphthalene being unaffected and the remaining components showing different degrees of response (Figure 6). Overall, the recommended dosing of SD25 (1:30 SD25:oil ratio, 333.3 mg SD25 l^{-1}) increased the W_i of most hydrocarbons. Crude and model oil concentrations followed an exponentially decaying trend with depth in the percentage of mass of TPHs retained in the sediment. SD25 application resulted in increased mobility of model oil through sediments but not in the relative amount of oil in the washout. In contrast, SD25 application resulted in an increase (from zero) in the percentage of crude oil present in the washout.

4.2 Sediment properties and Superdispersant-25 CMC

The sands used in this experiment were highly permeable (4×10^{-11} m^2, Table 3) and values were in agreement with prior characterisation of the estuary's sands (Zetsche et al., 2011). High permeability in the top 10 cm results in advective pore-water fluxes being the dominant transport mechanism of solutes (Huettel et al., 2014). Consequently, oil deposition on these permeable sands may result in significant hydrocarbon entrainment after an oil spill. This was evidenced here, where oil entrained the permeable sands beyond 10 cm deep (Figure 6) and is undesirable because sediment-entrained oil can persist for years (Lindeberg et al., 2017).

The apparent CMC of SD25 was calculated to be 21.1 mg l^{-1} (Figure 3), which is close to that reported for Corexit EC9500A (22.5 mg l^{-1}), a dispersant widely used during *DwH* (Gong et al. 2014), suggesting that the surfactant effect of the dispersants may be similar. The relevance of the CMC has been subject to extensive study within remediation and oil spill science in recent years. The desired effects of dispersant are frequently found above the CMC (Ahn et al., 2010; Gong et al., 2014; Zhao et al., 2015). Here, a similar response for SD25 was found for heptadecane and tetracosane leading to increased percolation over 10 cm at SD25 concentration = CMC (Figure 6). It has been shown that different commercial dispersants can have different effectiveness on spilt oil deposition. For example, Corexit dispersants accelerate settling of oil-mineral aggregates more effectively than SPC1000 (Cai et al., 2017). Furthermore, Corexit

390   dispersants promote photodegradation whereas SPC1000 inhibits it (Fu et al., 2016). It is
391   therefore important to establish the effects of dispersants such as SD25, which are stored to
392   respond to potential oil spills across the world, to adequately assess the implications of their
393   use and subsequent consequences.

4.3 Model oil – Crude oil comparison

395   SD25 application resulted in increased mobility of model oil components but the effect on
396   Schiehallion crude oil was less consistent (Figure 4) This may have been due to the greater
397   complexity of crude oil composition (1000s of components) compared to that of the model oil
398   (21 components), which showed a distinct exponentially decreasing percentage retained at
399   increasing sediment depth. Additionally, the method used to establish TPHs for the
400   Schiehallion crude oil may be less robust than that used for the model oil (gravimetry vs. gas
401   chromatography, respectively). However, the use of a simpler oil (i.e. a model oil) facilitated
402   the interpretation of oil-dispersant interaction mechanisms in seawater and highlighted the need
403   for further research to understand the behaviour of multi-component mixtures in a multi-media
404   system such as the oil-dispersant-seawater-sediment system analysed in this work.

4.4 Hydrocarbon entrainment into the top 10 cm of sand

406   SD25 application had distinct effects on the mobility of hydrocarbons through permeable sands
407   (Figure 5). SD25 concentration below 42 mg SD25 l^{-1} had a relatively low impact on the
408   mobility of most hydrocarbons in the top 10 cm. The effect was most apparent at high SD25
409   concentration, indicating that SD25 concentration >150 mg l^{-1} may be necessary for
410   hydrocarbons to readily entrain into these sands. C_{10-12} entrainment showed a linear increase
411   with SD25 concentration (Figure 5). These components are of limited concern as they are
412   relatively volatile and are readily biodegraded (Liu and Liu, 2013). Longer-chained aliphatics
413   (C_{12+}) responded non-linearly but almost always monotonically to an increase in SD25
414   concentration (Figure 5). C_{14-16} were readily mobilised around 4 cm deep at the recommended
415   SD25 dosing compared to in its absence. This suggested that SD25 selectively mobilised
416   aliphatics with long chains more readily than those with short ones. Interestingly, the effect of
417   SD25 application on 1-octadecene entrainment was minimal compared to the C_{17} and C_{20}
418   saturate hydrocarbons of the model oil (Figure 5). A key difference which may influence 1-
419   octadecene's interactions with an oil-dispersant-seawater-sediment system with respect to C_{17}
420   and C_{20} saturate hydrocarbons is the presence of a double bond, promoting stronger adsorption
421   to sediment surfaces than saturates. Analogue comparisons between decane (C_{10} paraffin) and

422   1-decene (C_{10} olefin) reveal that entrainment of 1-decene is less pronounced than that of decane

423   in the top 4 cm of sediment but not deeper (Figure 5). This suggested that SD25 may be less

424   effective in mobilising olefins compared to paraffin. BTEX components showed a limited

425   increase in entrainment with SD25 concentration up to 150 mg l^{-1}, which agrees with previous

426   work on the limited effect of SD25 on the dissolution and dispersion of these components of

427   the model oil in seawater (Perez Calderon et al., 2018). These components were found in higher

428   (normalised) concentrations in the washout hydrocarbon-dispersant-water solution (Figure 6),

429   highlighting the capability of hydrocarbons to be entrained into coastal permeable sediments

430   beyond 10 cm and impact benthic ecosystems. SD25 recommended dosing (1:30 SD25:oil

431   ratio, in this work 333.3 mg l^{-1}) resulted in enhanced entrainment of BTEX components (Figure

432   5). However, unless an oil spill occurs nearshore, it is unlikely that these hydrocarbons will

433   reach coastal sediments due their high volatility and low K_{OW}. Nevertheless, BTEX have been

434   detected in coastal sediment (Phelps and Young, 1999) and consequently, following the

435   precautionary principle, these interactions should be considered in any dispersant application

436   decision-making process. Dispersant-facilitated adsorption has been shown for PAHs using the

437   dispersant Corexit 9500 (Gong et al., 2014; Zhao et al., 2015). In this work, PAHs showed a

438   similar response to C_{14+} aliphatics with an increase in hydrocarbon entrainment with SD25

439   concentration in the top 4 cm of sediment and the effect becoming more pronounced over 4 cm

440   deep. Dispersant application is typically carried out offshore where high-energy mixing can

441   take place with the aim of preventing beaching of spilled oil. However, dispersant can enhance

442   the entrainment into permeable sands by increasing the solubility of hydrocarbons and reducing

443   droplet size.

4.5   Hydrocarbon entrainment beyond 10 cm of sediment

445   Washout of hydrocarbons over 10 cm deep in Ythan estuary sands was enhanced by SD25

446   application for most hydrocarbons (Figure 6). Aliphatic hydrocarbons of specific chain length

447   ranges (C_{15-17} and C_{20-24}) increased their W_i with SD25 application. In contrast, the effect of

448   SD25 was less apparent on C_{10-14} and C_{18} aliphatics suggesting that SD25 may selectively

449   enhance the mobility of certain hydrocarbons in permeable sediments. C_{10-14} aliphatics are the

450   most soluble alkanes of the model oil and, therefore, a lesser impact of SD25 was expected.

451   Intertidal microbial communities play an important role in organic carbon processing in marine

452   sediments (Woulds et al., 2016). Facilitated entrainment of these hydrocarbons may result in

453   microbial community succession in intertidal permeable sands shifting the microbial

454   composition to hydrocarbon degrading communities (Lamendella et al., 2014). Furthermore,

bacterial oxidation of hydrocarbons may increase their water-solubility, making them more mobile within the sediment. The W_i of the most water-soluble hydrocarbons of the model oil (BTEX components and naphthalene) varied across the SD25 concentration range analysed and SD25 application did not have a consistent effect on the capacity of these hydrocarbons to entrain sands beyond 10 cm deep. This is may be due to their high water-solubilities which may limit the effect of SD25 application (Perez Calderon et al., 2018). Previous work has shown a reduced effect of dispersant application on the solubilisation of naphthalene, compared to pyrene (Zhao et al., 2015). This suggests that SD25 enhances the mobility of BTEX components and naphthalene into permeable sands but not their dissolution or dispersion in seawater, implying that pore-water transport of dissolved BTEX and naphthalene is less affected by dispersant application than that of larger, less seawater-soluble hydrocarbons. Larger PAHs (>2 rings) showed a similar response with low W_i values below 42 mg SD25 l^{-1}. However, there was an inflexion point between the CMC and 42 mg SD25 l^{-1} from which hydrocarbon entrainment increases for these PAHs, indicating that a threshold in enhancing solubility in water may exist for SD25 effectiveness on large PAHs. Dibenzothiophene showed a steady increase in W_i with SD25 concentration, indicating a different response to SD25 than the other PAHs. Dibenzothiophene was the only resin (contains sulphur in its structure) in the model oil, which may explain its higher W_i at low SD25 concentration. Overall, these results suggested that hydrocarbons within a mixture such as a crude oil entrain permeable sediments and solubilise to different extents and that dispersant application affected this process differently for specific groups of hydrocarbons.

5 Conclusions

This work highlighted the capability of a synthetic hydrocarbon mixture (model oil) and a crude oil (Schiehallion) to entrain permeable sands *via* natural percolation and the facilitation of this process by dispersant application. The main findings of the work were:

(1) A positive effect of SD25 concentration on hydrocarbon mobility was observed below the manufacturer's recommended dosing in permeable sands. Enhanced percolation beyond 10 cm deep was detectable at as low as SD25 CMC (21.1 mg l^{-1}).

(2) SD25 concentration increased the mobility of model oil through permeable sands and selectively mobilised larger hydrocarbon components (less water-soluble) than smaller components (more water-soluble) of the model oil.

486   (3) Both the model and Schiehallion crude oils readily entrained permeable North East
487   Scotland sands. The concentration profiles by depth followed an exponential decay
488   pattern for model oil but were poorly reproduced for crude oil, highlighting the
489   complexity of interactions in crude oil mobility through permeable media. SD25
490   application increased the entrainment of model oil but not of Schiehallion crude oil,
491   again due to high variability.

492 The findings of this work highlight the potential of oil to readily be entrained into permeable
493 sands in the event of an oil spill and that dispersant application exacerbates the process for
494 some oil components more than others. Further work is needed to understand how different
495 commercial dispersant formulations can affect oil entrainment and how this varies by oil,
496 hydrocarbon and sediment type as well as how seawater moves through sandy sediments and
497 potentially displaces hydrocarbons already present in them.

498   6   Acknowledgements

503   7   References

504 Ahn, C.K., Woo, S.H., Park, J.M., 2010. Selective adsorption of phenanthrene in nonionic–
505   anionic surfactant mixtures using activated carbon. Chem. Eng. J. 158, 115–119.
506   https://doi.org/10.1016/j.cej.2009.12.014

507 Balls, P.W., 1994. Nutrient Inputs to Estuaries from Nine Scottish East Coast Rivers; Influence
508   of Estuarine Processes on Inputs to the North Sea. Estuar. Coast. Shelf Sci. 39, 329–352.
509   https://doi.org/10.1006/ecss.1994.1068

510 Bandara, U.C., Yapa, P.D., Xie, H., 2011. Fate and transport of oil in sediment laden marine
511   waters. J. Hydro-environment Res. 5, 145–156. https://doi.org/10.1016/j.jher.2011.03.002

512 Beyer, J., Trannum, H.C., Bakke, T., Hodson, P. V., Collier, T.K., 2016. Environmental effects
513   of the Deepwater Horizon oil spill: A review. Mar. Pollut. Bull. 110, 28–51.
514   https://doi.org/10.1016/j.marpolbul.2016.06.027

515 Blott, S.J., Pye, K., 2001. GRADISTAT: a Grain Size Distribution and Statistics Package for
516   the Analysis of Unconsolidated Sediments. Earth Surf. Process. Landforms 26, 1237–
517   1248. https://doi.org/10.1002/esp.261

518 Cai, Z., Fu, J., Liu, W., Fu, K., O'Reilly, S.E.E., Zhao, D., 2017. Effects of oil dispersants on
519   settling of marine sediment particles and particle-facilitated distribution and transport of
520   oil components. Mar. Pollut. Bull. 114, 408–418.
521   https://doi.org/10.1016/j.marpolbul.2016.09.057

522 Cleveland, W.S., Grosse, E., Shyu, W.M., 1992. Local regression models, in: Chambers, J.M.,
523   Hastie, T.J. (Eds.), Statistical Models in S. Wadsworth & Brooks/Cole.

524 Davies, J.M., Tibbetts, P.J.C., 1987. The use of in situ benthic chambers to study the fate of oil
525   in sublittoral sediments. Estuar. Coast. Shelf Sci. 24, 205–223.
526   https://doi.org/10.1016/0272-7714(87)90065-5

527 Ferguson, R.M.W., Gontikaki, E., Anderson, J.A., Witte, U., 2017. The Variable Influence of
528   Dispersant on Degradation of Oil Hydrocarbons in Subarctic Deep-Sea Sediments at Low
529   Temperatures (0–5 °C). Sci. Rep. 7, 2253. https://doi.org/10.1038/s41598-017-02475-9

530 Fingas, M.F., 2002. A review of literature related to oil spill dispersants especially relevant to
531   Alaska. Prince William Sound Reg. citizens Advis. Counc. Anchorage, Alaska.

532 Fu, J., Gong, Y., Cai, Z., O'Reilly, S.E., Zhao, D., 2016. Mechanistic investigation into
533   sunlight-facilitated photodegradation of pyrene in seawater with oil dispersants. Mar.
534   Pollut. Bull. 114, 751–758. https://doi.org/10.1016/j.marpolbul.2016.10.077

535 Gong, Y., Zhao, X., O'Reilly, S.E., Qian, T., Zhao, D., 2014. Effects of oil dispersant and oil
536   on sorption and desorption of phenanthrene with Gulf Coast marine sediments. Environ.
537   Pollut. 185, 240–249. https://doi.org/10.1016/j.envpol.2013.10.031

538 Hazen, T.C., Dubinsky, E. a, DeSantis, T.Z., Andersen, G.L., Piceno, Y.M., Singh, N., Jansson,
539   J.K., Probst, A., Borglin, S.E., Fortney, J.L., Stringfellow, W.T., Bill, M., Conrad, M.E.,
540   Tom, L.M., Chavarria, K.L., Alusi, T.R., Lamendella, R., Joyner, D.C., Spier, C., Baelum,
541   J., Auer, M., Zemla, M.L., Chakraborty, R., Sonnenthal, E.L., D'haeseleer, P., Holman,
542   H.-Y.N., Osman, S., Lu, Z., Van Nostrand, J.D., Deng, Y., Zhou, J., Mason, O.U., 2010.
543   Deep-Sea Oil Plume Enriches Indigenous Oil-Degrading Bacteria. Science (80-.). 330,
544   204–208. https://doi.org/10.1126/science.1195979

545   Head, H.K., 1982. Manual of soil laboratory testing, Vol 2. Pentech Press.

546   Huettel, M., Berg, P., Kostka, J.E., 2014. Benthic Exchange and Biogeochemical Cycling in
547   Permeable Sediments. Ann. Rev. Mar. Sci. 6, 23–51. https://doi.org/10.1146/annurev-
548   marine-051413-012706

549   International Association of Oil & Gas Producers, 2015. Dispersants : subsea application Good
550   practice guidelines for incident management and emergency response personnel.

551   Lamendella, R., Strutt, S., Borglin, S., Chakraborty, R., Tas, N., Mason, O.U., Hultman, J.,
552   Prestat, E., Hazen, T.C., Jansson, J.K., 2014. Assessment of the Deepwater Horizon oil
553   spill impact on Gulf coast microbial communities. Front. Microbiol. 5, 130.
554   https://doi.org/10.3389/fmicb.2014.00130

555   Leach, J.H., 1971. Hydrology of the Ythan Estuary With Reference to Distribution of Major
556   Nutrients and Detritus. J. Mar. Biol. Assoc. United Kingdom 51, 137.
557   https://doi.org/10.1017/S0025315400006536

558   Levine, B.M., White, J.R., DeLaune, R.D., 2017. Impacts of the long-term presence of buried
559   crude oil on salt marsh soil denitrification in Barataria Bay, Louisiana. Ecol. Eng. 99,
560   454–461. https://doi.org/10.1016/j.ecoleng.2016.11.017

561   Lindeberg, M.R., Maselko, J., Heintz, R.A., Fugate, C.J., Holland, L., 2017. Conditions of
562   persistent oil on beaches in Prince William Sound 26 years after the Exxon Valdez spill.
563   Deep Sea Res. Part II Top. Stud. Oceanogr. https://doi.org/10.1016/j.dsr2.2017.07.011

564   Liu, Z., Liu, J., 2013. Evaluating bacterial community structures in oil collected from the sea
565   surface and sediment in the northern Gulf of Mexico after the Deepwater Horizon oil spill.
566   Microbiologyopen 2, 492–504. https://doi.org/10.1002/mbo3.89

567   Nixon, Z., Zengel, S., Baker, M., Steinhoff, M., Fricano, G., Rouhani, S., Michel, J., 2016.
568   Shoreline oiling from the Deepwater Horizon oil spill. Mar. Pollut. Bull. 107, 170–178.
569   https://doi.org/10.1016/j.marpolbul.2016.04.003

570   Paramor, O.A.L., Allen, K.A., Aanesen, M., Armstrong, C., Hegland, T., Le Quesne, W.,
571   Raakaer, G.J., Roger, S., van Hal, R., van Hoof, L.J.W., van Overzee, H.M.J., Frid, C.L.J.,
572   2009. MEFEPO North Sea Atlas, University of Liverpool.

573   Payne, J.R., Driskell, W.B., Short, J.W., Larsen, M.L., 2008. Long term monitoring for oil in
574   the Exxon Valdez spill region. Mar. Pollut. Bull. 56, 2067–2081.

575   https://doi.org/10.1016/j.marpolbul.2008.07.014

576   Perez Calderon, L. J., Potts, L. D., Gontikaki, E., Gubry-Rangin, C., Cornulier, T., Gallego, A.,
577   Anderson, J., Witte, U. (2018). Bacterial Community Response in Deep Faroe-Shetland
578   Channel Sediments Following Hydrocarbon Entrainment With and Without Dispersant
579   Addition. Frontiers in Marine Science, 5. https://doi.org/10.3389/fmars.2018.00159

580   Phelps, C.D., Young, L.Y., 1999. Anaerobic biodegradation of BTEX and gasoline in various
581   aquatic sediments. Biodegradation 10, 15–25. https://doi.org/10.1023/A:1008303729431

582   Prince, R.C., 2015. Oil spill dispersants: Boon or bane? Environ. Sci. Technol. 49, 6376–6384.
583   https://doi.org/10.1021/acs.est.5b00961

584   R Development Core Team, 2017. R: A language and environment for Statistical computing.
585   R Found. Stat. Comput.

586   Ramseur, J., 2010. Deepwater Horizon oil spill: the fate of the oil.

587   White, H.K., Hsing, P.-Y., Cho, W., Shank, T.M., Cordes, E.E., Quattrini, A.M., Nelson, R.K.,
588   Camilli, R., Demopoulos, A.W.J., German, C.R., Brooks, J.M., Roberts, H.H., Shedd, W.,
589   Reddy, C.M., Fisher, C.R., 2012. Impact of the Deepwater Horizon oil spill on a deep-
590   water coral community in the Gulf of Mexico. Proc. Natl. Acad. Sci. 109, 20303–20308.
591   https://doi.org/10.1073/pnas.1118029109

592   Wickham, H., 2009. ggplot2: Elegant Graphics for Data Analysis.

593   Widdel, K., Knittel, A., Galushko, F., 2010. Anaerobic Hydrocarbon- Degrading
594   Microorganisms: An Overview, in: Timmis, N.K., McGenity, T., Meer, J.R., Lorenzo, V.
595   (Eds.), Handbook of Hydrocarbon and Lipid Microbiology. pp. 1997–2022.
596   https://doi.org/10.1007/978-3-540-77587-4

597   Wood, S., 2011. Mixed GAM Computation Vehicle with GCV/AIC/REML smoothness
598   estimation and GAMMs by REML/PQL.

599   Wood, S., 2006. Low rank scale invariant tensor product smooths for generalized additive
600   mixed models. Biometrics 62, 1025–1036.

601   Woulds, C., Bouillon, S., Cowie, G.L., Drake, E., Middelburg, J.J., Witte, U., 2016. Patterns
602   of carbon processing at the seafloor: The role of faunal and microbial communities in
603   moderating carbon flows. Biogeosciences 13, 4343–4357. https://doi.org/10.5194/bg-13-

604   4343-2016

605   Zetsche, E., Paterson, D.M., Lumsdon, D.G., Witte, U., 2011. Temporal variation in the
606   sediment permeability of an intertidal sandflat. Mar. Ecol. Prog. Ser. 441, 49–63.
607   https://doi.org/10.3354/meps09390

608   Zhao, X., Gong, Y., O'Reilly, S.E., Zhao, D., 2015. Effects of oil dispersant on solubilization,
609   sorption and desorption of polycyclic aromatic hydrocarbons in sediment–seawater
610   systems. Mar. Pollut. Bull. 92, 160–169. https://doi.org/10.1016/j.marpolbul.2014.12.042

611   Zuijdgeest, A., Huettel, M., 2012. Dispersants as Used in Response to the MC252-Spill Lead
612   to Higher Mobility of Polycyclic Aromatic Hydrocarbons in Oil-Contaminated Gulf of
613   Mexico Sand. PLoS One 7, e50549. https://doi.org/10.1371/journal.pone.0050549

614